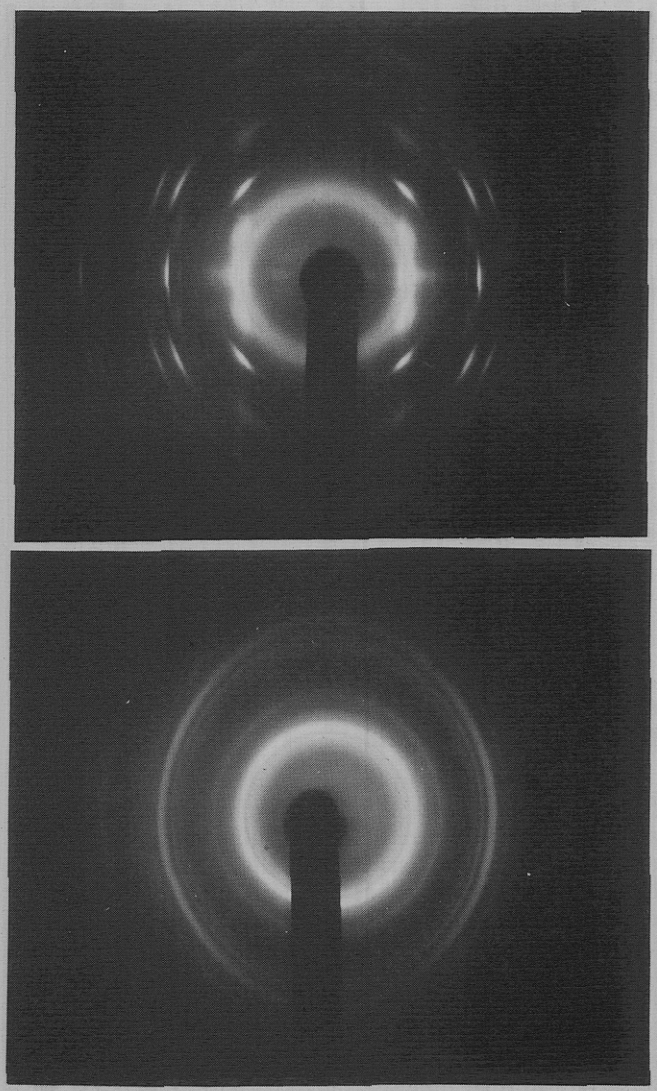

Figure 1. (Top) Fiber diagram of form III of poly(vinylidene fluoride). (Bottom) X-ray diffraction pattern of unoriented form III.

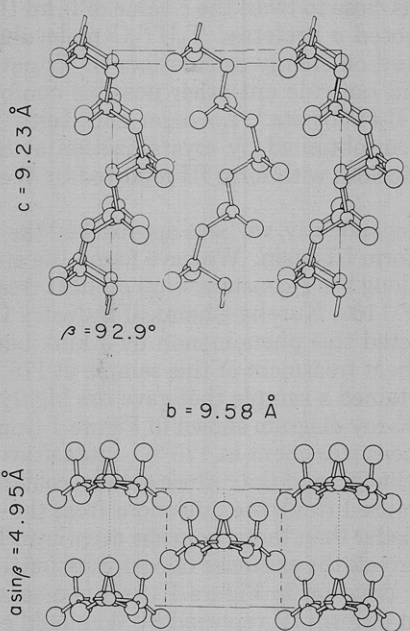

Figure 2. Crystal structure of form III of poly(vinylidene fluoride).

tion, drying in vacuo, and annealing at 175 °C for about 1 h.

All of the observed reflections were indexed by a monoclinic unit cell with parameters $a = 4.96$ Å, $b = 9.58$ Å, c (fiber axis) = 9.23 Å, and $\beta = 92.9°$. The systematic absences $h + k \neq 2n$ for hkl and $l \neq 2n$ for $h0l$ suggested that space groups Cc and $C2/c$ be examined. We considered the $T_3GT_3\bar{G}$ and $(TG)_2(T\bar{G})_2$ conformations, which have fiber identity periods of 9.11 and 8.78 Å, respectively, as plausible molecular models.

After applying repeated trial and error and constrained least-squares methods,[9,10] we obtained the crystal structure shown in Figure 2. The space group is Cc-C_s^4 and the molecular conformation is essentially the $T_3GT_3\bar{G}$ type. The R factor is 17% for the 47 independent reflections. The agreement between the observed and calculated intensities is better in the even-number layers than in the odd-number layers. This fact may be associated with some disorder. The structure is polar as in the case of form I. Piezoelectricity should be expected.

Form II showing streaks could be obtained by heat treatment of form II. Furthermore, formation of the fiber diagram, which coincides with form III on the even-number layers and which gives streaks along the ξ-constant lines on the odd-number layers, depends on sample preparation. This suggests that form II continuously transforms into form III via the form II that shows streaks, and the form II with the streaks is characterized as an intermediate phase between forms II and III. During the transformation, the molecular conformation continuously changes from $TGT\bar{G}$ to $T_3GT_3\bar{G}$ by flip-flop motions.[8] Accordingly, this transition is not considered to be of the first order but of higher order.

References and Notes

(1) R. Hasegawa, M. Kobayashi, and H. Tadokoro, *Polym. J.*, **3**, 591 (1972).
(2) R. Hasegawa, Y. Takahashi, Y. Chatani, and H. Tadokoro, *Polym. J.*, **3**, 600 (1972).
(3) S. Weinhold, M. H. Litt, and J. B. Lando, *J. Polym. Sci., Polym. Lett. Ed.*, **17**, 585 (1979).
(4) M. A. Bachmann, W. L. Gordon, J. L. Koenig, and J. B. Lando, *J. Appl. Phys.*, **50**, 6106 (1979).
(5) S. K. Tripathy, R. Potenzonne, Jr., A. J. Hopfinger, N. Banik, and P. L. Taylor, *Macromolecules*, **12**, 656 (1979).
(6) A. J. Lovinger and H. D. Keith, *Macromolecules*, **12**, 919 (1979).
(7) Y. Takahashi, M. Kohyama, and H. Tadokoro, *Macromolecules*, **9**, 870 (1976).
(8) Y. Takahashi and H. Tadokoro, *Macromolecules*, preceding paper in this issue.
(9) S. Arnott and A. J. Wonacott, *Polymer*, **7**, 157 (1966).
(10) Y. Takahashi, T. Sato, H. Tadokoro, and Y. Tanaka, *J. Polym. Sci., Polym. Phys. Ed.*, **11**, 233 (1973).

Yasuhiro Takahashi and Hiroyuki Tadokoro*
Department of Macromolecular Science
Faculty of Science, Osaka University
Toyonaka, Osaka 560, Japan

Received May 1, 1980

Kink Bands in Form I of Poly(vinylidene fluoride)[1]

In previous papers,[2,3] it was reported that the X-ray diffuse streak scatterings found on the fiber diagram of form II of poly(vinylidene fluoride) are attributable to kink bands which are one monomeric unit thick and are mainly formed by the flip-flop motion between the $TGT\bar{G}$ and $T\bar{G}TG$ conformations. An X-ray diffuse streak scattering was also found on the fiber diagram of form I of poly(vinylidene fluoride). Here, we report that this X-ray diffuse streak scattering is also attributable to kink bands contained in the crystallite of form I.

A fiber specimen of form I was prepared by stretching at room temperature after the melt (KF-1100, Kureha

0024-9297/80/2213-1318$01.00/0

Chemical Industry Co., Ltd.) was quenched in ice water. On the fiber diagram of form I (Figure 1), an X-ray diffuse streak scattering is observed on the line connecting the overlapped reflections of 110 and 200 with the reflection 001. This shows that, in reciprocal space, the diffuse streak scattering extends from the 001 reflection to either the 110 or 200 reflection. In general, the presence of diffuse streak scattering suggests that disorder exists in a crystallite having, in the plane perpendicular to the extending direction of the diffuse streak scattering, the same two-dimensional periodicity as the regular lattice. Accordingly, by analogy with the kink bands of form II and, moreover, from the extending direction of the diffuse streak scattering, the disorder is also inferred to be kink bands which are formed parallel to either of the two sets of planes {111} or {201}. Here, a set of {111} planes consists of four equivalent planes (111), ($\bar{1}11$), ($1\bar{1}1$), and ($\bar{1}\bar{1}1$), and {201} consists of (201) and ($\bar{2}01$).

The molecular conformation in form I is essentially planar zigzag.[4] Therefore, the kink bands in form I should be formed by introducing G or $\bar{G}$ conformations into the planar zigzag conformation. Here, two models were considered for the molecular conformation in the kink bands: one is $GT_n\bar{G}$ (n = odd) and the other is a repetition of the $TGT\bar{G}$ conformation. These two molecular models were used in building kink-band models parallel to two sets of planes, {111} and {201}, and the molecular packing in the kink bands was examined. From the van der Waals contact, only the kink bands parallel to {111} were possible; kink bands parallel to {201} were not allowed because interatomic distances are too short. Accordingly, the diffuse streak scattering is considered to be on a line connecting the reflections 110 and 001 in reciprocal space.

The intensity distribution along the X-ray diffuse streak scattering was calculated for two kink-band models parallel to {111} by using the intensity equation for stacking faults:[5-7] the kink bands are of the $GT_n\bar{G}$ (n = odd) conformation in model I and of $TGT\bar{G}$ repetition in model II. When the kink bands are formed parallel to one of a set of {111} planes and the hydrogen atoms are ignored, the structure of form I containing the kink bands can be constructed by two kinds of unit-layer structures A and B, which are one monomeric unit thick and have infinite size on the plane parallel to one of a set of planes {111}. Models I and II can be described by stacking of the unit-layer structures A and B and by stacking of layer structures A and AB, respectively (Figure 2). Here, the layer structure AB was made by putting the unit-layer structure B on the unit-layer structure A. By assuming that the existence probability of the unit-layer structure A (w_A) is equal to 0.9, the number of parameters can be reduced to one, P_{ij}, where P_{ij} is the probability of finding layer j after layer i. The intensity distribution calculation was made for various values of P_{ij}. The calculated intensity distribution curves for models I and II, which agree well with the intensity distribution observed on the fiber diagram, are shown in Figure 3 along with the value of P_{ij}. Here, the intensity was divided by the radial coordinate ξ in reciprocal space in order to compare with the intensity distribution on the fiber diagram. On the observed diffuse streak scattering from 001 to 110 (Figure 1), the intensity gradually decreases after a steep descent near the 001 reflection, and at about one-quarter it reaches a minimum. After the minimum, the intensity gradually increases and finally it merges into the halo due to the amorphous region around the middle of the two reflections. The maximum on the calculated intensity distributions would not be observed because of the halo. Both of the calculated intensity distributions reproduce the observed distribution

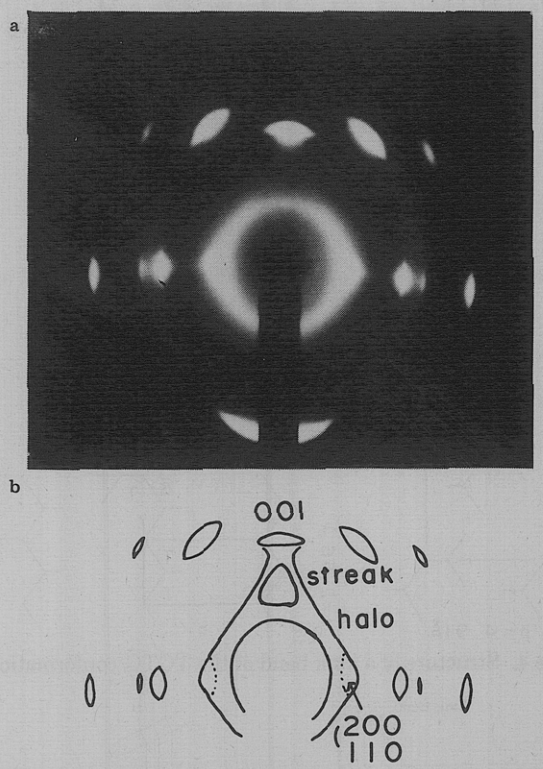

Figure 1. (a) Fiber diagram of form I and (b) its schematic representation. The fiber axis is tilted by about 17.5°.

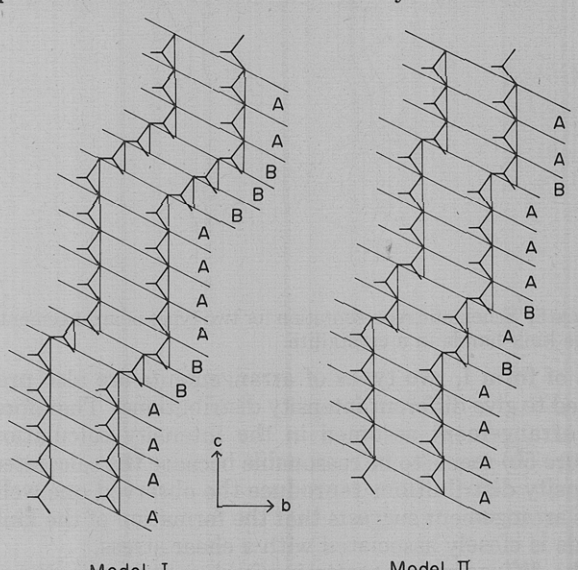

Figure 2. Two kink-band models and two unit-layer structures A and B.

well. This elucidates the existence of the kink bands in the crystallite of form I, although it cannot indicate which model is correct. The kink band composed of $TGT\bar{G}$ is shown in Figure 4.

The intensity distribution calculation was made on the assumption that the kink bands were parallel to one of a set of {111} planes (Figure 5b). From the extending direction of the diffuse streak scattering, another type of arrangement could be considered, where the kink bands parallel to all of the {111} planes coexist in a crystallite (Figure 5a). The intensity calculation was not made for this arrangement because the intensity equation for stacking faults could not be applied. However, in the case of form II,[3] the calculation was made for the models in which the regular segments shift perpendicular to the chain axis in a corresponding manner (models II and IV in ref 3), giving quite different intensity distributions. In the

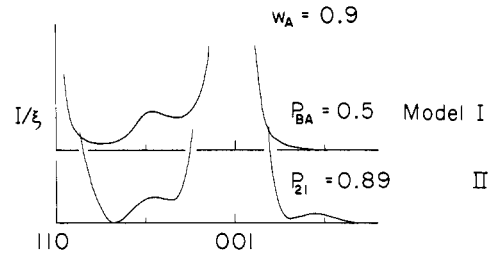

Figure 3. Calculated intensity distributions for models I and II.

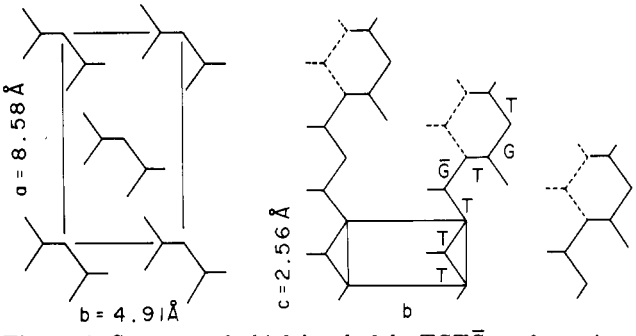

Figure 4. Structure of a kink band of the TGT$\bar{G}$ conformation.

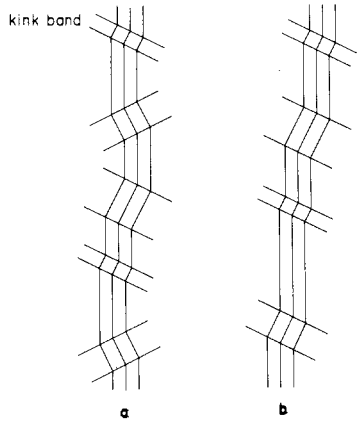

Figure 5. Schematic representation for two types of arrangements of the kink bands in a crystallite.

case of form I, two types of arrangements are also presumed to give different intensity distributions. Therefore, the arrangement assumed in the intensity calculation (Figure 5b) seems to be reasonable because the calculated intensity distributions reproduce the observed one well. This arrangement suggests that the formation of the kink bands is closely associated with a shear stress.

The diffuse streak scattering is observed generally on the fiber diagram of form I prepared by stretching unoriented form II. Accordingly, two mechanisms can be considered for the formation of the kink bands: (1) the TGT$\bar{G}$ conformation of form II remains, in part, after the transformation to form I and it forms a band in the crystallite of form I and (2) the kink bands are formed in the crystallite of form I by a shear stress after the transformation to form I. The kink bands in form II appear as an intermediate structure between forms II and III, arising from the flip-flop motion during the heat treatment.[3,8] However, it seems likely that the kink bands of the planar zigzag conformation also may be introduced into the crystallite of form II by a shear stress. Accordingly, the transformation from form II to form I is considered to be a kind of martensitic transformation. In other words, a shear stress forms the kink bands of the planar zigzag structure in the crystallite of form II, the kink bands grow in thickness, and, finally, form I results from the self-diffusion of the molecules into each stable position. From this consideration, the first mechanism seems to play an important role. In both mechanisms, the kink bands in form I result from a shear stress applied to the ends of the crystallite during the deformation process in contrast to the kink bands in form II. Furthermore, the formation of the kink bands may be associated with the transformation of form II to form I on stretching.

References and Notes

(1) Presented in part at the IUPAC International Symposium on Macromolecules, Mainz, 1979.
(2) Y. Takahashi, M. Kohyama, and H. Tadokoro, *Macromolecules*, **9**, 870 (1976).
(3) Y. Takahashi and H. Tadokoro, *Macromolecules*, in press.
(4) R. Hasegawa, Y. Takahashi, Y. Chatani, and H. Tadokoro, *Polym. J.*, **3**, 600 (1972).
(5) J. Kakinoki and Y. Komura, *J. Phys. Soc. Jpn.*, **9**, 169 (1954).
(6) G. Allegra, *Acta Crystallogr.*, **17**, 579 (1964).
(7) K. Yoshida, *J. Phys. Soc. Jpn.*, **35**, 482 (1973).
(8) Y. Takahashi and H. Tadokoro, *Macromolecules*, in press.

Yasuhiro Takahashi* and Hiroyuki Tadokoro

Department of Macromolecular Science
Faculty of Science, Osaka University
Toyonaka, Osaka 560, Japan

Akira Odajima

Department of Applied Physics
Faculty of Engineering, Hokkaido University
Sapporo 060, Japan

Received May 5, 1980

Application of High-Resolution ^{13}C NMR Spectroscopy Using Magic Angle Spinning Techniques to the Direct Investigation of Solid Cured Phenolic Resins

Phenolic resins, formed from the reaction of phenol with formaldehyde, were among the very first completely synthetic polymers made[2] (Bakelite) and still find very wide commercial applications.[3]

The reaction is carried out under two general types of reaction conditions as indicated in Schemes I and II.

In both cases the final polymers are highly cross-linked, giving considerable mechanical strength to articles fabricated from them. Reaction under alkaline conditions yields a product which contains methylene bridges, dibenzyl ether linkages, and free methylol (CH_2OH) groups. Under acidic conditions the condensation product contains methylene bridges. However, conclusions regarding the structure of the final cured products are by inference only, as the high degree of cross-linking which gives them their useful mechanical properties also renders them completely insoluble in all solvents. Application of most analytical techniques to the determination of their structures is not practical, although IR spectroscopy has had limited success, being able to distinguish methylol from dibenzyl ether groupings from their C–O stretching frequencies.[4]

In recent years it has been shown that a combination of cross-polarization,[5] high-power decoupling, and magic angle spinning techniques[6] can be used to obtain high-resolution ^{13}C NMR spectra of solid materials, and a number of such studies have indicated the power and versatility of this technique.[7-9] The technique is particularly useful in the application to resins and other solid materials which are insoluble.[10] The present communication describes in outline the potential application of these techniques to the determination of the structures of solid phenolic resins and related compounds. Spectra were recorded on a Bruker CXP 100 spectrometer by using the

0024-9297/80/2213-1320 $01.00/0